Molecular Microbiology (2014) 94(3), 609–624 ■
doi:10.1111/mmi.12782
First published online 19 September 2014

Two essential FtsH proteases control the level of the Fur repressor during iron deficiency in the cyanobacterium *Synechocystis* sp. PCC 6803

Vendula Krynická,[1,2] Martin Tichý,[1,2] Jaroslav Krafl,[1] Jianfeng Yu,[3] Radek Kaňa,[1,2] Marko Boehm,[3] Peter J. Nixon[3] and Josef Komenda[1,2]*

[1]*Institute of Microbiology, Academy of Sciences, Opatovický mlýn, 37981 Třeboň, Czech Republic.*
[2]*Faculty of Science, University of South Bohemia, Branišovská 31, 370 05 České Budějovice, Czech Republic.*
[3]*Department of Life Sciences, Sir Ernst Chain Building-Wolfson Laboratories, Imperial College London, South Kensington Campus, London SW7 2AZ, UK.*

Summary

The cyanobacterium *Synechocystis* sp. PCC 6803 expresses four different FtsH protease subunits (FtsH1-4) that assemble into specific homo- and heterocomplexes. The FtsH2/FtsH3 complex is involved in photoprotection but the physiological roles of the other complexes, notably the essential FtsH1/FtsH3 complex, remain unclear. Here we show that the FtsH1 and FtsH3 proteases are involved in the acclimation of cells to iron deficiency. A mutant conditionally depleted in FtsH3 was unable to induce normal expression of the IsiA chlorophyll-protein and FutA1 iron transporter upon iron deficiency due to a block in transcription, which is regulated by the Fur transcriptional repressor. Levels of Fur declined in the WT and the FtsH2 null mutant upon iron depletion but not in the FtsH3 downregulated strain. A similar stabilizing effect on Fur was also observed in a mutant conditionally depleted in the FtsH1 subunit. Moreover, a mutant overexpressing FtsH1 showed reduced levels of Fur and enhanced accumulation of both IsiA and FutA1 even under iron sufficiency. Analysis of GFP-tagged derivatives and biochemical fractionation supported a common location for FtsH1 and FtsH3 in the cytoplasmic membrane. Overall we propose that degradation of the Fur repressor mediated by the FtsH1/FtsH3 heterocomplex is critical for acclimation to iron depletion.

Accepted 30 August, 2014. *For correspondence. E-mail komenda@alga.cz; Tel. (+420) 384 340431; Fax (+420) 384 340415.

Introduction

The membrane-embedded FtsH proteases found in bacteria as well as in chloroplasts and mitochondria contain an AAA+ (ATPase associated with diverse cellular activities) module, a Zn^{2+}-binding protease domain (Erzberger and Berger, 2006) and form oligomeric complexes involved in a number of cellular functions including protein quality control, transcriptional regulation and organelle biogenesis. The genome of the cyanobacterium *Synechocystis* sp. PCC 6803 (hereafter *Synechocystis* 6803) encodes four FtsH homologues designated FtsH1-4. FtsH1, encoded by the *slr1390* gene, and FtsH3, encoded by the *slr1604* gene, are crucial for cell viability whereas FtsH2, encoded by the *slr0228* gene, and FtsH4, encoded by the *sll1463* gene, are dispensable proteins (Mann *et al.*, 2000). FtsH2 forms a heterohexameric complex with FtsH3 (Boehm *et al.*, 2012) and is involved in photosystem II (PSII) repair (Silva *et al.*, 2003) and in general quality control of PSII in the thylakoid membrane of *Synechocystis* 6803 (Komenda *et al.*, 2006; Nixon *et al.*, 2010). Pull-down experiments have also provided evidence for the formation of an FtsH4 homocomplex and another FtsH heterocomplex consisting of the FtsH1 and FtsH3 subunits (Boehm *et al.*, 2012), but the location, subunit organization and function of this FtsH1/FtsH3 complex remain to be clarified. Since previous results (Wegener *et al.*, 2010) and our own preliminary experiments indicated a large increase in the levels of FtsH1, FtsH2 and FtsH3 upon iron depletion (Fig. 1), we have focused in this paper on their possible involvement in the acclimation to iron deficiency.

Iron is an essential element for all bacteria because of its role as a cofactor for enzymes involved in cellular metabolism. Although abundant in the environment, iron deficiency frequently occurs due to oxidation of the ferrous ion to the ferric ion which is highly insoluble at physiological pH (Breitbarth *et al.*, 2010; Ratledge and Dover, 2000). While iron limitation has obvious consequences, bacteria also have to maintain a tight control over iron acquisition, because free intracellular iron can react with superoxide

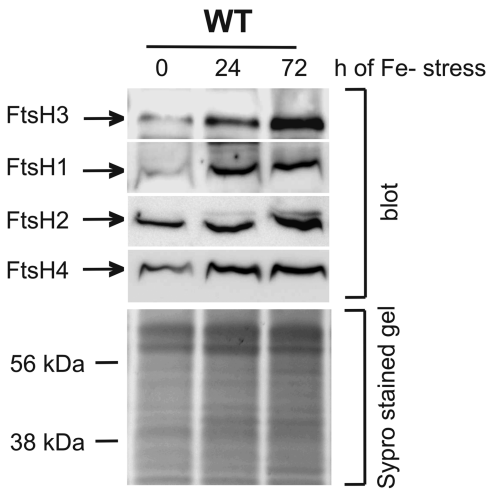

Fig. 1. Level of FtsH proteases in WT under iron deficiency. Thylakoid membranes isolated from WT cells harvested after 0, 24 and 72 h of growth under iron depletion were analysed by 1D SDS-PAGE, gels were stained by Sypro Orange and used for immunodetection using antibodies specific for FtsH1-4 proteases. Part of the Sypro stained gel is shown to document loading of the samples. Each loaded sample contained 2 μg of Chl.

and hydrogen peroxide forming highly reactive hydroxyl radicals (Guerinot and Yi, 1994). In cyanobacteria iron is also essential for the photosynthetic electron transport chain as it is a constituent of many proteins involved in electron transport. Thus cyanobacterial iron homeostasis is tightly controlled, both at the protein level through incorporation of free metal ions into metallo-proteins (Lewin *et al*., 2005), and more importantly at the transcriptional level through the regulated expression of genes encoding metal trafficking proteins, including uptake and storage proteins (Ghassemian *et al*., 2006; Hernández-Prieto *et al*., 2012). Iron deficiency results in a variety of physiological and morphological changes in cyanobacteria (Leonhardt and Straus, 1994). It causes significant loss of the light-harvesting phycobilisomes (Guikema and Sherman, 1983), reduction in the Photosystem I (PSI) content (Sherman and Sherman, 1983), and replacement of proteins with iron-containing cofactors by those with non-iron cofactors, such as flavodoxin for ferredoxin (Laudenbach *et al*., 1988). Moreover, this stress results in significant changes in fluorescence and absorption properties of the cells: a blue shift of the chlorophyll (Chl) absorbance peak measured at room temperature (shift from 677–679 nm to 670–671 nm), and a large increase in the Chl fluorescence emission peak at 685 nm measured at 77 K. These spectral changes directly correlate with expression of the *isiA* gene encoding a Chl-binding protein that is homologous to PsbC, the CP43 inner antenna protein of Photosystem II (PSII) (Burnap *et al*., 1993; Bibby *et al*., 2001a). In *Synechocystis* 6803 IsiA functions as a Chl storage protein and/or as an antenna for PSI (Bibby *et al*., 2001b; Singh and Sherman, 2007). Studies suggest that regulation of *isiA* is controlled at both the transcriptional and post-transcriptional level. Post-transcriptional regulation is mediated by an antisense RNA molecule, IsrR, transcribed from the *isiA* non-coding strand (Dühring *et al*., 2006). However, the main regulation of *isiA* expression is at the level of transcription which is under the control of the ferric uptake regulator, Fur (Ghassemian and Straus, 1996; Kunert *et al*., 2003).

Fur is a widespread bacterial protein that regulates the expression of iron-uptake and iron-storage systems in response to intracellular iron concentration (Crosa, 1997; Escolar *et al*., 1999; Dian *et al*., 2011; González *et al*., 2012). It acts as a transcriptional repressor in the presence of iron, which functions as a co-repressor to increase the binding affinity of Fur for AT-rich DNA elements termed Fur-boxes, present in the core promoters of iron-regulated genes (Escolar *et al*., 1997; Escolar *et al*., 1999; Yu and Genco, 2012). However, at low iron concentrations iron-free Fur (apo-Fur) has a reduced affinity for the Fur-boxes allowing the RNA polymerase to access the promoters of the downstream genes to initiate transcription (Bagg and Neilands, 1987; Hernández *et al*., 2006). Whether the level of the iron-free form of Fur is subject to proteolytic control has not been addressed.

In the genome of *Synechocystis* 6803 there are three genes coding for Fur-like proteins. One of them, encoded by the *slr1738* gene, seems to be a functional homologue of the peroxide-sensing PerR protein (Li *et al*., 2004; Garcin *et al*., 2012). Another one, encoded by *sll1937*, is a zinc-uptake regulator, Zur (Hantke, 2001; Tottey *et al*., 2012), whereas the third Fur-like protein, Sll0567, is a likely true functional Fur homologue.

In this study we present evidence that the proteolytic FtsH1/FtsH3 heterocomplex is located in the cytoplasmic membrane of *Synechocystis* 6803 and regulates transcription of iron depletion-induced genes by controlling the availability of the transcriptional regulator Fur (Sll0567). When expression of each of the two FtsH subunits forming the FtsH1/FtsH3 heterocomplex was conditionally suppressed, the corresponding mutants maintained a high level of Fur during iron starvation and lost the ability to acclimate via activation of *isiA* transcription. On the other hand, overexpression of FtsH1 resulted in the decreased cellular level of Fur and the accumulation of IsiA even in cells cultivated under standard iron concentrations.

Results

A Synechocystis *strain with suppressed expression of the FtsH3 protease does not accumulate IsiA during iron starvation*

To establish a possible physiological role of FtsH3 in acclimation to iron starvation we used the previously

constructed and characterized SynFtsH3down strain of *Synechocystis* 6803 (Boehm *et al*., 2012) (hereafter FtsH3down) lacking the chromosomal copy of *ftsH3* but containing a plasmid-borne copy of *ftsH3*. Expression of this gene is driven by the *nirA* promoter, the activity of which is dependent on the concentration of NH_4^+ ions in the cultivation medium (Qi *et al*., 2005; Boehm *et al*., 2012). The presence of 13 mM NH_4^+ in the medium led to the parallel loss of FtsH3, FtsH2 and FtsH1 within 5 days (Boehm *et al*., 2012), whereas their disappearance was not observed in WT cultivated under identical conditions (hereafter WT_{NH4+}) (Fig. S1). At this point FtsH3down as well as WT_{NH4+} cells were transferred to a medium lacking iron and containing the iron chelator deferoxamine (DFB). To test whether FtsH2 (and hence the FtsH2/FtsH3 heterocomplex) is also involved in acclimation to iron depletion, the experiment was also performed with a mutant lacking the FtsH2 protease grown in the presence of ammonia ($FtsH2^-_{NH4+}$). Within 24 h of iron depletion, the spectral properties of WT_{NH4+} and $FtsH2^-_{NH4+}$ cells exhibited symptoms of acclimation to iron depletion, namely a blue shift of the Chl absorption peak from 679 nm for WT_{NH4+} and 676 nm for $FtsH2^-_{NH4+}$, respectively, to 673 nm. After 72 h of iron depletion the Chl absorption peak shifted to 670 nm for both strains and then its value remained unchanged (Fig. 2A). In contrast to WT_{NH4+} and $FtsH2^-_{NH4+}$, the FtsH3down mutant exhibited no spectral changes typical for iron starvation (Fig. 2A). After 24, 72 and even 120 h (not shown) the Chl absorbance peak maximum remained at 678 nm.

All changes observed in WT_{NH4+} and $FtsH2^-_{NH4+}$ cells in the presence of DFB have been previously ascribed to the iron deficiency-induced disappearance of PSI and accumulation of the IsiA protein which becomes the major Chl-binding protein of iron-starved cells of *Synechocystis* 6803 (Singh and Sherman, 2007). To confirm that the same phenomena occurred in WT_{NH4+} and $FtsH2^-_{NH4+}$ but not in FtsH3down, we analysed proteins of all three strains by one- and two-dimensional (1D and 2D) PAGE in combination with immunoblotting. Although the Chl/OD_{750} ratio decreased in all strains during iron depletion due to changed optical properties of the cells, the Chl/protein ratio remained constant. Therefore, all samples were loaded on an equal Chl basis; identical results were obtained when loading was performed on an equal protein basis. A 1D-stained gel together with immunodetection (Fig. 2B) clearly showed that WT_{NH4+} and $FtsH2^-_{NH4+}$ accumulated IsiA and another iron-depletion induced protein FutA1 after 72h of iron depletion while in the FtsH3down mutant IsiA and FutA1 were hardly detectable as determined by immunoblotting and by staining combined with mass spectrometry respectively (see Table 1). The amount of PSI core protein PsaA also clearly decreased in the first two strains (Fig. 2B) while its content remained

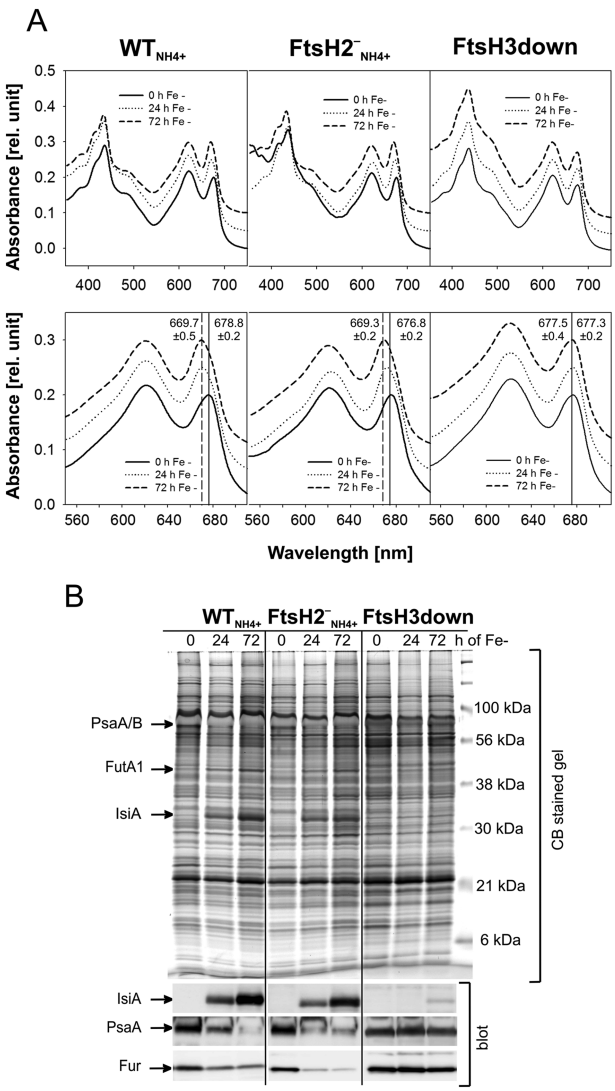

Fig. 2. Whole cell absorption spectra (A) and membrane protein content (B) during acclimation of WT_{NH4+}, $FtsH2^-_{NH4+}$ and FtsH3down strains to iron starvation. Cultures grown in BG11 medium containing 13 mM ammonium chloride were transferred to iron depleted medium supplemented with 10 μM deferoxamin and cells were harvested after 0, 24 and 72 h of iron depletion for assessment.
A. Absorption spectra were measured with cell suspensions of OD_{750} of 0.1. They were normalized to the red Chl absorption peak (670–680 nm) and then spectra after 24 h (dotted lines) and 72 h (dashed lines) were shifted by 0.05 and 0.1 A, respectively, for better visualization of differences. A magnified absorption region 550 – 700 nm is also shown with vertical lines designating absorption maxima and numbers showing the mean of absorption maxima from three biological replicates ± SE.
B. Membranes isolated from harvested cells were analysed by 1D SDS-PAGE; gels were either stained by Coomassie Blue (CB stained gel) or were used for immunodetection of IsiA, PsaA and Fur. IsiA and FutA1 were also identified by mass spectrometry (see Table 1). Each loaded sample contained 2 μg of Chl.

Table 1. List of proteins identified by a combination of 2D CN/SDS PAGE, mass spectrometry and immunoblotting in the cells of control and iron-depleted cells.

	Mass spectrometric analysis				
Protein UniProtKB No.	Size (Da) Length (AA)	Coverage (%)	Detected/theoretical no. of peptides	PLGS score	Immunoblot
CP47 P05429	55 903 507	38	16/28	2409	+
CP43 P09193	50 303 460	33	11/25	1934	+
D2 P09192	39 466 352	24	7/14	1350	+
D1 P16033	39 695 360	20	6/14	1051	+
IsiA Q55274	37 221 342	20	6/15	785	+
FutA1 P72827	39 370 360	19	5/21	645	–
PsaA P29254	82 950 751	–	–	–	+
PsaD P19569	15 644 141	32	2/9	56	+

PLGS score is a statistical measure of peptide assignment accuracy.

almost unchanged in the FtsH3down strain. A similar conclusion could also be made from a 2D analysis of membrane proteins which showed accumulation of FutA1 and various forms of IsiA protein ranging from monomeric protein to trimeric PSI-IsiA supercomplexes in cells of WT_{NH4+} and $FtsH2^{-}_{NH4+}$ depleted of iron for 72 h (Figs 3 and S2). Both strains also showed the disappearance of most of the PSI trimer and PSI monomer due to their conversion into PSI-IsiA supercomplexes (Fig. S2, PsaD). Interestingly, the control cells contained a low level of PSII dimer and high level of carotenoids (Fig. 2A) before the start of iron depletion, which is probably related to the adverse effects of ammonia (Drath *et al.*, 2008). After addition of DFB the amount of PSII dimer increased (Fig. 3) and carotenoid content was lowered (Fig. 2A) indicating that iron depletion partly relieved cells from the ammonia-induced stress. In contrast to WT_{NH4+} and $FtsH2^{-}_{NH4+}$ cells, the FtsH3down mutant grown under identical conditions contained no detectable FutA1 and IsiA-containing complexes; instead the level of PSII dimer further decreased after addition of the chelator and absorption spectra showed a small additional increase in the level of carotenoids (Fig. 2A).

FtsH3down cannot upregulate isiA *transcription under iron deficiency due to a high level of Fur repressor*

Previous studies of iron starvation in cyanobacteria showed a strong correlation between the accumulation of IsiA and the level of its transcript (Singh and Sherman, 2000; Singh *et al.*, 2003; Shcolnick *et al.*, 2009). To examine whether the FtsH3 protease is involved in this transcriptional regulation, we assessed the level of *isiA* transcript in cells of all three studied strains before and after incubation with DFB. The transcript level was estimated by reverse transcription-PCR (RT-PCR). The amount of *isiA* transcript was similar for all three strains when grown in medium with the standard iron concentration. However, after 24 h of iron depletion it increased almost fifty times in WT_{NH4+} and $FtsH2^{-}_{NH4+}$ cells while in FtsH3down cells it increased maximally twice (Fig. 4). After 72 h of iron starvation the difference in the *isiA* expression among the tested strains was much smaller reaching about seven to nine times the initial level in WT_{NH4+} and $FtsH2_{NH4+}$ and five times in FtsH3down. The large increase in the *isiA* transcript after 24 h followed by the drop after 72 h was consistently observed in WT_{NH4+} cells, but has not been detected in previous transcriptomic studies, possibly because of differences in how iron was depleted from the cells. Here we used a combination of iron–free medium and DFB chelator whereas previous studies used either iron-deficient media without iron chelator (Singh *et al.*, 2003), or normal media with chelator (Hernández-Prieto *et al.*, 2012), conditions that might deplete iron from the cells more slowly. In summary, the data on the changes in the *isiA* transcript level during iron depletion corresponded to the observed accumulation of the IsiA and FutA1 proteins found in the individual strains.

The level of the *isiA* transcript is determined by its half-life which is affected by antisense RNA (Dühring *et al.*, 2006) and the rate of transcription which is mostly dependent on binding of the Fur repressor (Ghassemian and Straus, 1996; Kunert *et al.*, 2003; González *et al.*,

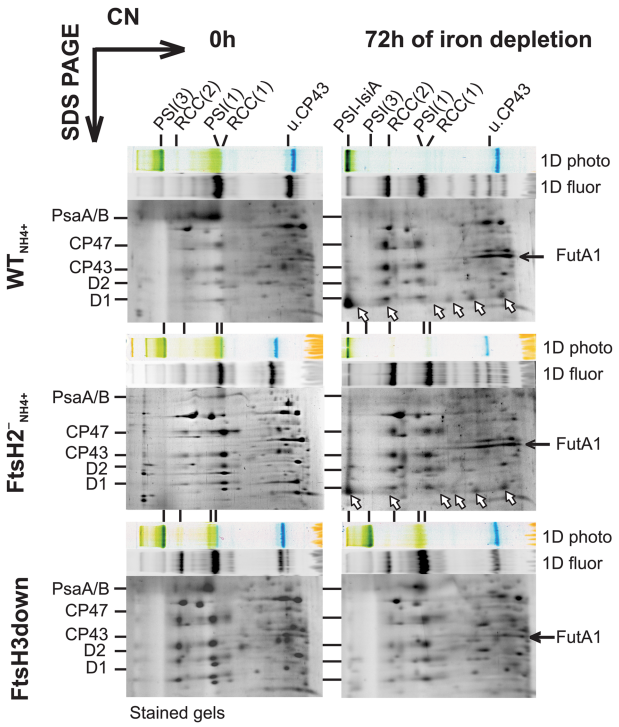

Fig. 3. Accumulation of membrane protein complexes in cells of WT_{NH4+}, $FtsH2^{-}_{NH4+}$ and FtsH3down strains before and after 72 h of iron depletion. Cells grown in BG11 medium containing 13 mM ammonium chloride were transferred to iron-depleted medium supplemented with 10 μM deferoxamin B. Thylakoid membranes were isolated from cells harvested after 0 and 72 h of growth in iron depleted medium containing 10 μM deferoxamin B. Membrane protein complexes were analysed by 2D CN/SDS-PAGE. The 1D native gel was photographed (1D photo) or scanned by LAS 4000 for fluorescence (1D fluor) and after SDS-PAGE in the 2nd dimension the resulting 2D gel was stained by Sypro Orange. Each loaded sample contained 5 μg of Chl. Designation of complexes: PSI(3) and PSI(1), trimeric and monomeric Photosystem I complexes; PSI-IsiA, supercomplexes of trimeric Photosystem I and IsiA; RCC(2) and RCC(1), dimeric and monomeric Photosystem II core complexes; u.CP43, unassembled CP43. White arrows designate IsiA protein in various complexes, black arrows FutA1. The identity of FutA1 was verified by mass spectrometry (see Table 1), IsiA by immunoblotting (Fig. S2).

2012). As FtsH2 has been implicated in regulation of another transcriptional regulator, NdhR, in *Synechocystis* 6803 (Zhang *et al.*, 2007), we were interested whether FtsH3 could participate in regulating the levels of the Fur repressor. Using a Fur-specific antibody (Fig. S3A) we detected the vast majority of Fur in the membrane fraction of *Synechocystis* cells (Fig. S3C) and during iron depletion the level of Fur significantly decreased in membranes of both WT_{NH4+} and $FtsH2^{-}_{NH4+}$ while no such decrease was observed in FtsH3down (Fig. 2B). Analysis of the soluble fractions revealed that in WT_{NH4+} the protein became almost undetectable after 72 h of iron deficiency while the soluble fraction of the mutant contained even more Fur than at the beginning (Fig. S3C).

To confirm that the iron-responsive changes in the Fur level were not affected by the presence of ammonia, we also checked the level of Fur in the membrane fraction isolated from WT cultivated in the iron-depleted standard BG11 medium. Again, the abundance of the IsiA transcript steeply increased (Fig. 5A) and corresponded to a strong decrease in the amount of Fur during 72 h of iron starvation (Fig. 5B).

The presence of Fur in the membrane fraction of *Synechocystis* was rather surprising and was therefore investigated in more detail in WT membranes. Most of the Fur protein was released from membranes by treatment with 0.1 M Na_2CO_3 confirming that Fur is not a trans-membrane protein (Fig. 6). Surprisingly, when membranes were solubilized by the mild detergent dodecylmaltoside (DDM), which we routinely use to solubilize membranes for CN-PAGE, the Fur protein remained almost exclusively in the unsolubilized fraction while the D1 protein of PSII and PilA1 were easily solubilized. Neither the iron chelator DFB nor the nuclease benzonase improved solubilization of the protein by DDM. Only in the presence of EDTA was a large portion of the protein released suggesting the role of divalent cations in the attachment of Fur to membranes (Fig. 6).

To further support the effect of FtsH3 on Fur-regulated gene expression, we also assessed the amount of transcript from the *slr1295* gene which codes for the FutA1 ferric ion transporter which we observed over-accumulated in both 1D and 2D electrophoretic gels in iron-deficient WT_{NH4+} and $FtsH2^{-}_{NH4+}$ but not in FtsH3down (Fig. 2B; Fig. 3). This gene has been shown to be upregulated during iron deficiency (Hernández-Prieto *et al.*, 2012) and belongs to operons included in the Regulog collection of

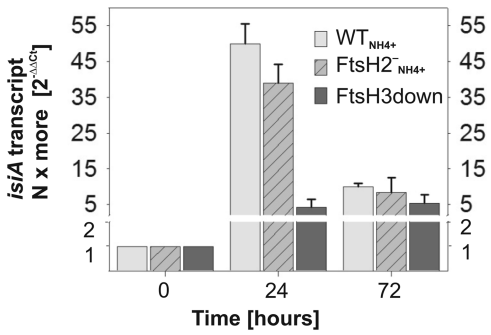

Fig. 4. *isiA* transcript level in WT_{NH4}, $FtsH2^{-}_{NH4+}$ and FtsH3down cells. Amount of the *isiA* transcript was measured by RT-PCR method. $2^{-\Delta\Delta Ct}$ means a multiple of the initial transcript level after indicated time of iron depletion when the initial level for each strain is set to one ($2^{-\Delta\Delta Ct} = 1$). *RnpB* was used as a reference gene. The initial levels of the transcript in $FtsH2^{-}_{NH4+}$ and FtsH3down were reaching 150 and 80% of that in WT_{NH4+} respectively; means of 3 independent measurements ± SD are plotted.

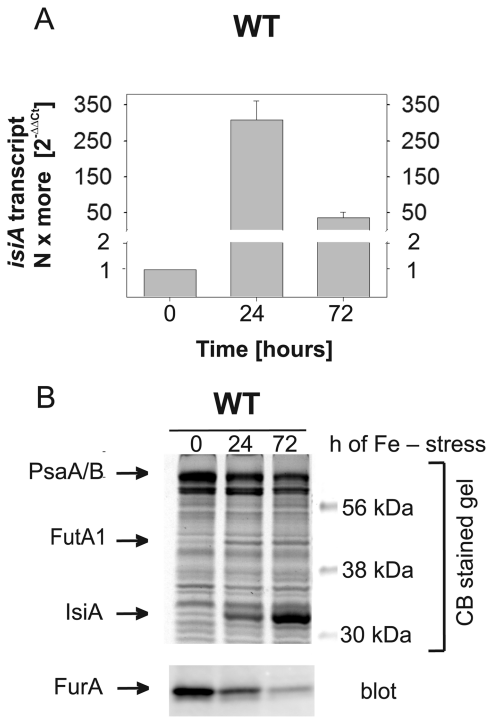

Fig. 5. *isiA* transcript level and content of the Fur repressor in control WT cells untreated with ammonia during iron depletion.
A. Amount of the *isiA* transcript was measured by RT-PCR method. $2^{-\Delta\Delta Ct}$ means a multiple of the initial transcript level after indicated time of iron depletion when the initial level is set to one ($2^{-\Delta\Delta Ct} = 1$). *RnpB* gene was used as a reference gene. Means of 3 independent measurements ± SD are plotted.
B. Membranes isolated from the cells harvested after 0, 24 and 72 h of iron depletion were analysed by 1D SDS-PAGE; gels were either stained by Coomassie Blue (CB stained gel) or used for immunodetection of Fur. Each loaded sample contained 2 μg of Chl which is within the linear range for detecting Fur as documented in Fig. S3B.

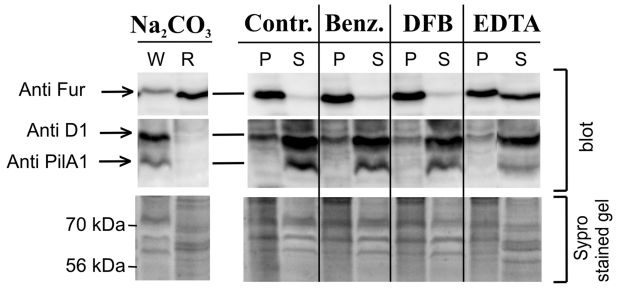

Fig. 6. Characterization of Fur membrane association in WT cells. The membrane fraction isolated from the cells of WT was treated in the following way before analysis by 1D SDS-PAGE:
Na_2CO_3 – membrane fraction washed with 0.1M Na_2CO_3 pH 12; W – washed membranes, R – released proteins; Contr. – control membrane fraction solubilized by 1% DDM; Benz. – membrane fraction solubilized by 1% (w/v) DDM in the presence of 60 U benzonase; DFB – membrane fraction solubilized by 1% (w/v) DDM in the presence of 250 μM DFB; EDTA – membrane fraction solubilized by 1% (w/v) DDM in the presence of 25 mM EDTA. P means pellet; S means supernatant after solubilization by 1% (w/v) DDM. The gels were stained by Sypro Orange for control of loading and used for immunodetection by antibodies specific for Fur, D1 and PilA1. Each loaded membrane sample contained 1.5 μg of Chl, with the amount of loaded supernatant corresponding to 1.5 μg of Chl of the membrane fraction.

genes putatively regulated by Fur (http://regprecise.lbl.gov/RegPrecise/genome.jsp?genome_id=305). Indeed, the result confirmed that the increase in the level of *slr1295* transcript after iron depletion was strongly suppressed in FtsH3down similar to the IsiA transcript (Fig. 7).

Manipulating the level of FtsH1 affects the cellular level of IsiA regardless of iron concentration

FtsH3 was recently identified as a component of the FtsH2/FtsH3 heterohexameric complex responsible for quality control of PSII in the thylakoid membrane (Boehm *et al.*, 2012). Since our present data showed that the FtsH2-less strain is not impaired in acclimation to iron depletion, the FtsH2/FtsH3 complex could be ruled out from participating in the regulation of Fur levels. Given the current lack of experimental support for the existence of FtsH3 homo-oligomeric complexes and our previous data supporting the existence of FtsH1/FtsH3 heterocomplexes (Boehm *et al.*, 2012) plus the present results showing the role of FtsH3 in regulation of Fur levels, we hypothesized that the FtsH1/FtsH3 complex is responsible for this regulation and that manipulating the level of FtsH1 should also affect the acclimation to iron deficiency. To test this hypothesis we constructed two new *Synechocystis* 6803 mutants differing in the cellular content of the FtsH1 protease. The strain FtsH1down was constructed similarly to FtsH3down by inserting the *ftsH1* gene under a regulatable promotor, in this case the promotor of the *petJ* gene encoding

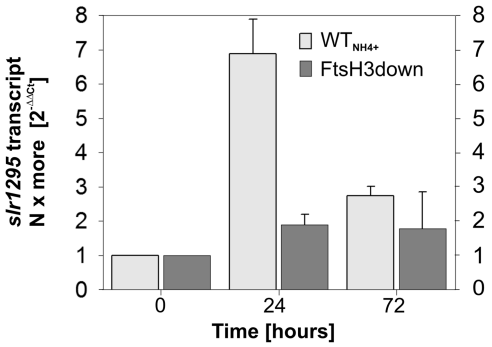

Fig. 7. Transcript levels of *slr1295* gene regulated by Fur in WT_{NH4+} and FtsH3down during iron depletion. Transcripts were measured by RT-PCR method. $2^{-\Delta\Delta Ct}$ means a multiple of the initial transcript level after indicated time of iron depletion when the initial level for each strain is set to one ($2^{-\Delta\Delta Ct} = 1$). *RnpB* gene was used as a reference gene. The initial level of the transcript in FtsH3down was reaching 98 % of that in WT_{NH4+}. Measurements were performed in triplicate using independent cultures; means ± SD are plotted.

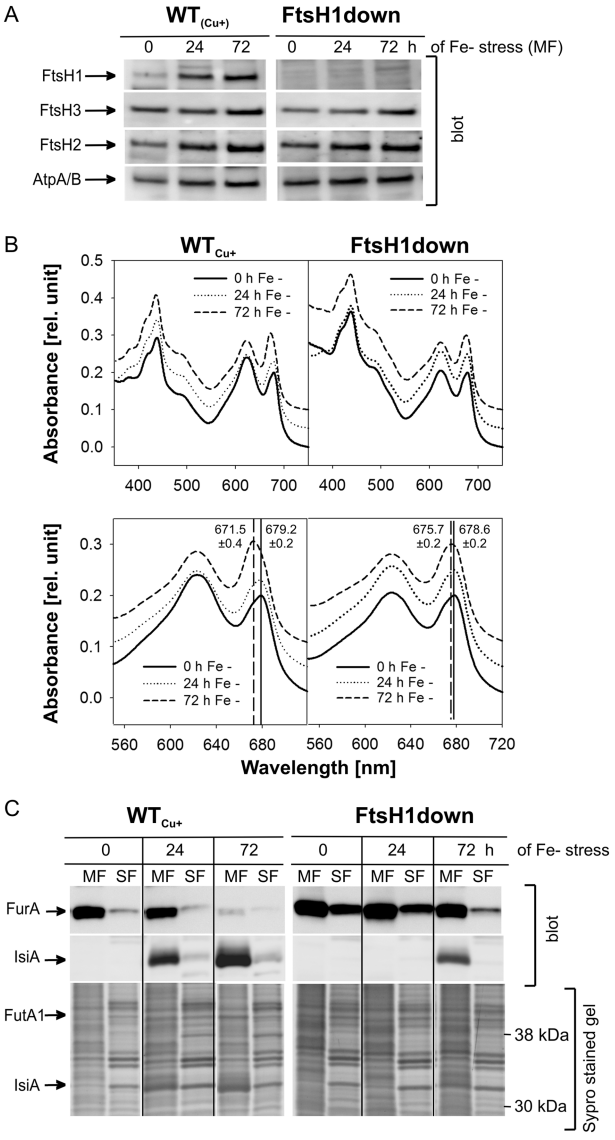

Fig. 8. Changes in the FtsH levels (A), whole cell absorption spectra (B) and content of IsiA, FutA1 and Fur (C) during acclimation of WT_{Cu+} and FtsH1down strains to iron starvation. Cultures of WT and FtsH1down grown in the BG11Cu+ medium were transferred to iron depleted medium containing 10 μM deferoxamin B and cells were harvested after 0, 24 and 72 h of iron depletion for assessment.
A. Membrane proteins isolated from cells of WT_{Cu+} and FtsH1down after 0, 24 and 72 h of iron depletion were analysed by 1D SDS-PAGE and immunoblot using antibodies against FtsH1, FtsH2 and FtsH3. The non-specific staining of AtpA/B subunits of ATP synthase is also shown to document loading of the lanes. Each loaded sample contained 2 μg of Chl.
B. Absorption spectra were measured with cell suspensions of the same OD_{750} of 0.1 that were normalized to the red Chl absorption peak (673–679 nm). Spectra after 24 h (dotted lines) and 72 h (dashed lines) were shifted by 0.05 and 0.1 A, respectively, for better visualization of differences. A magnified absorption region 550 – 700 nm is also shown with vertical lines designating the mean of absorption maxima from three biological replicates ± SE.
C. Membrane (MF) and soluble (SF) fractions isolated from the cells harvested after 0, 24 and 72 h of iron depletion were analysed by 1D SDS-PAGE, gels were stained by Sypro Orange and used for immunodetection of Fur and IsiA. Identity of FutA1 and IsiA in the stained gel was verified by mass spectrometry. Each loaded sample of MF contained 2 μg of Chl; amount of loaded SF corresponded to amount of membrane containing 2 μg of Chl.

cytochrome c_6, which is downregulated in the presence of copper ions (Tous *et al.*, 2001; Kuchmina *et al.*, 2012). Copper-induced suppression of FtsH1 was not as effective as suppression of FtsH3 in FtsH3down using the *nirA* promoter; nevertheless the *ftsH1* transcript level in the absence of Cu^{2+} (before suppression) was four times lower in comparison to control WT cells and after 8 days of cultivation in the presence of 0.8 μM Cu^{2+} the transcript level declined six times in comparison to WT. In this copper-enriched medium the FtsH1 protein became almost undetectable by immunodetection and its negligible level was maintained even when grown under iron depletion (Fig. 8A). On the other hand, the amount of FtsH1 in the control cells of WT_{Cu+} increased after 72 h of iron depletion. Similar to FtsH3down after DFB treatment, the FtsH1-down mutant exhibited retardation in IsiA accumulation in comparison to WT_{Cu+}. After 72 h of iron depletion the mutant cells showed only limited decrease in the phycobiliprotein content (Fig. 8B, region 600 –650 nm) and the Chl absorption maximum shifted from 678 nm to just 675 nm (Fig. 8B). This was reflected by the largely reduced level of IsiA protein when compared to WT_{Cu+} (Fig. 8C). Significantly, FtsH1down, like the FtsH3down mutant, accumulated higher levels of total Fur protein in comparison to WT_{Cu+} even before iron starvation and its level in both membrane and soluble fractions was reduced only slightly when compared to WT_{Cu+} after 72 h of iron starvation (Fig. 8C).

The second mutant, termed FtsH1over, contained eight times more *ftsH1* transcript than WT. This FtsH1 overexpression was achieved by inserting the *ftsH1* gene under the control of the promoter of the *psbA2* gene which encodes the D1 protein and which under standard growth conditions is the source of 90% of the cellular *psbA* transcript (Mohamed *et al.*, 1993). The mutant cells showed increased level of carotenoids, a lower content of phycobilisomes and a change in the shape of the red absorption maximum of Chl indicating increase in the absorption around 672 nm (Fig. 9A). Protein analysis of the mutant grown in the standard BG11 medium confirmed an increased content of FtsH1 and FtsH3 and showed accumulation of the IsiA protein (Fig. 9B) which was mostly present in PSI-IsiA complexes similar to those seen in the WT cells treated with DFB for 24 h (Fig. 9C). More importantly, the content of Fur protein was significantly lower in this strain in comparison with WT grown in normal BG11 medium (Fig. 9B). Overall our data indicate that both FtsH1

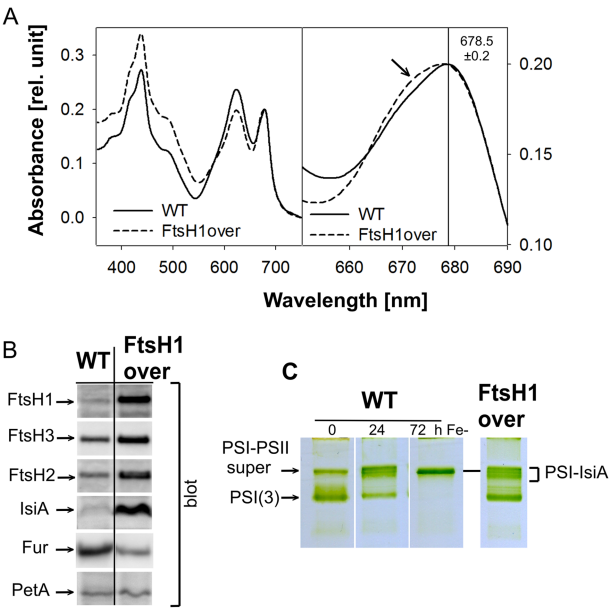

Fig. 9. Whole cell absorption spectra (A), content of FtsH1, FtsH2, FtsH3, IsiA and Fur proteins (B) and PSI-IsiA complexes (C) in the FtsH1over strain overexpressing FtsH1. Cultures of WT and FtsH1over were grown in standard BG11 medium.
A. Absorption spectra were measured with cell suspensions of the same OD_{750} of 0.1 that were normalized to the red Chl absorption peak (673–679 nm). A magnified absorption region 650–690 nm is also shown with the arrow designating the subtle difference in the Chl absorption between WT and FtsH1over due to the accumulation of IsiA.
B. Membranes isolated from harvested cells were analysed by 1D SDS-PAGE; gels were used for immunodetection of FtsH1, FtsH2, FtsH3, IsiA and Fur using specific antibodies. Chemiluminescent signal of cytochrome f (PetA) is also shown to document equal loading of the samples. Each loaded sample contained 2 μg of Chl.
C. Comparison of high molecular weight regions of the CN gel between FtsH1over and WT cells harvested after 0, 24 and 72 h of iron depletion. PSII-PSI supercomplexes present in the WT cells before iron depletion are overlapped by PSI-IsiA complexes with concomitant disappearance of trimeric PSI (PSI(3)) during iron depletion. Similar levels of PSI(3) and PSI-IsiA complexes are seen in the FtsH1over and WT cells depleted of iron for 24 h.

and FtsH3, most probably in the form of a heterooligomeric complex, are involved in the accumulation of Fur.

The FtsH1/FtsH3 complex is located in the cytoplasmic membrane

To further confirm the existence of the FtsH1/FtsH3 complex in *Synechocystis* 6803 we compared the amounts of each subunit in various mutant strains and assessed their co-migration on 2D gels. Previously we have reported that most of the FtsH2/FtsH3 complex migrates on native gels with an apparent molecular mass of 650 kDa. This mass is significantly higher than the size of 410 kDa predicted for a hexamer with the difference possibly reflecting the presence of additional protein components in the complex *in vivo* (Boehm *et al.*, 2012). In an FtsH2$^-$/FtsH4$^-$ double mutant (lacking both the FtsH2 and FtsH4 homologues) we detected a smaller 550-kDa complex using specific antibodies against FtsH1 and FtsH3. This complex was also found in WT together with a 650-kDa complex assigned to FtsH2/FtsH3. In contrast, the 550-kDa complex was not present in the FtsH1down strain. This result is consistent with our assumption that in the FtsH1down mutant the FtsH3 subunit is present only in the FtsH2/FtsH3 complex and that the 550-kDa complex can be assigned to the FtsH1/FtsH3 complex (Fig. 10). Overall, these data provide further support for the existence of an FtsH1/FtsH3 heterocomplex *in vivo*.

We have previously shown that FtsH2 and hence the FtsH2/FtsH3 complex is located in thylakoid membranes (Komenda *et al.*, 2006). To help determine the location of the FtsH1/FtsH3 complex we constructed mutants containing the GFP protein attached to the C-terminus of the FtsH1 and FtsH3 homologues (Fig. S7) and examined these strains by confocal fluorescence microscopy. As a control we used a strain having GFP attached to the C-terminus of FtsH2. The GFP-tagged FtsH subunits accumulated in the membranes as proteins of the expected size with only very limited fragmentation detected (Fig. S8). In addition all mutant strains could segregate indicating that the GFP-tagged FtsH1 and FtsH3 subunits were still functional *in vivo* and therefore the strains could be used for localization experiments. Figure 11 showing the distribution of Chl and GFP fluorescence in cells of all three strains clearly indicated a different pattern of GFP signal distribution. While in FtsH2-GFP the signal of Chl significantly overlapped with the signal of GFP, in the FtsH1-GFP mutant the signal of GFP was present on the surface of the cells clearly outside the Chl fluorescence. The signal of FtsH3-GFP overlapped thylakoids but also reached the cellular surfaces outside the Chl–containing thylakoids in agreement with its dual localization in both types of membranes. These results are

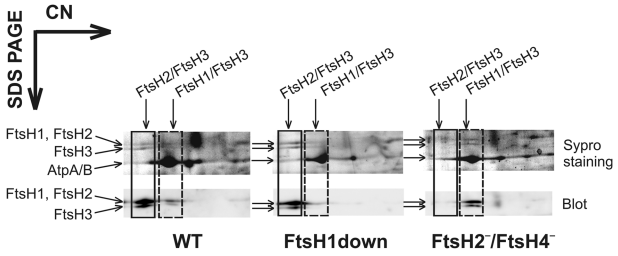

Fig. 10. FtsH3 forms separate hetero-oligomeric complexes with FtsH2 as well as with FtsH1 in *Synechocystis* 6803. Membranes of WT, FtsH1down and FtsH2$^-$/FtsH4$^-$ were analysed by 2D CN/SDS-PAGE in combination with immunodetection using antibodies specific for FtsH1-3. 5 μg of Chl were loaded in each lane of the first dimension. Solid rectangle delimits FtsH2/FtsH3 complex, dashed rectangle defines FtsH1/FtsH3 complex. Subunits α and β of the complete ATP synthase (AtpA/B) complex are also shown as internal standard for size estimation of the FtsH complexes.

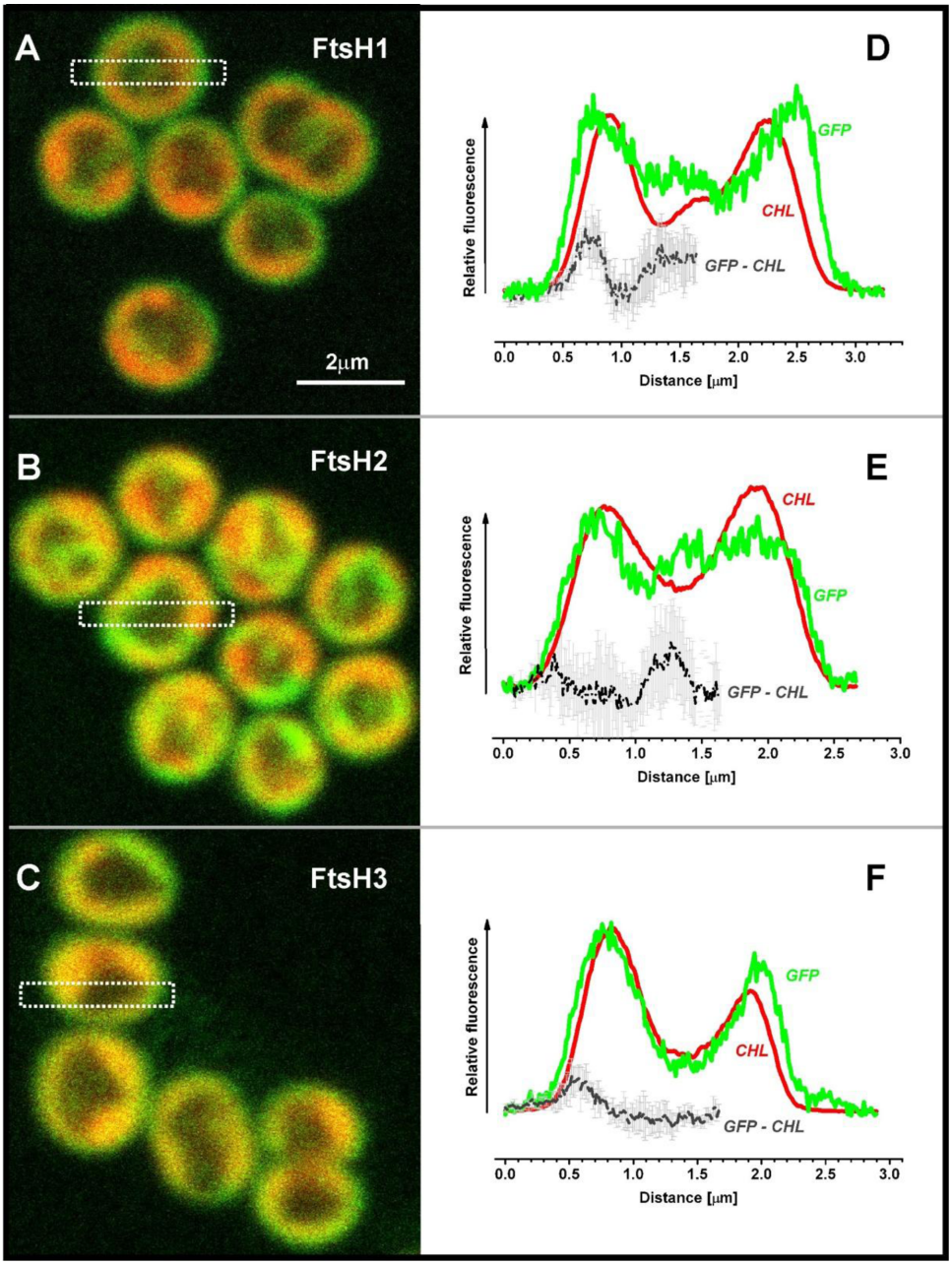

Fig. 11. Cellular localization of Chl fluorescence and GFP-tagged FtsH proteases in *Synechocystis* 6803. Panels A, B and C represent confocal microscopy images of *Synechocystis* 6803 cells containing GFP-tagged FtsH1, FtsH2 and FtsH3 proteases respectively. Green channel represents GFP fluorescence (excitation at 488 nm, detection at 500–530 nm), Chl emission is shown in red (excitation at 488 nm, detection at 690–790 nm). The presented pictures were used for further analysis of GFP-tagged FtsH proteases and Chl fluorescence (see D, E and F). Fluorescence intensity profiles across the *x*-axis of cells (see white bar) are presented (*GFP* – green line) together with localization of Chl emission in thylakoid membranes (*CHL* – red line), the profiles are normalized to fluorescence intensity of GFP and Chl at a distance value of 0.7 μm. Relative difference between GFP and Chl fluorescence (*GFP* – *CHL* – black line) represent averages and SD (grey) for 4 cells.

in line with a previous investigation by mass spectrometry of purified cytoplasmic and thylakoid membranes prepared by a combination of sucrose-gradient centrifugation and two-phase separation according to method of Huang *et al.* (2002). FtsH3 was detected in both membranes while FtsH1 was found just in the cytoplasmic membrane fraction (Pisareva *et al.*, 2007; 2011). We repeated this separation procedure with WT cells and using an immunoblotting approach confirmed the localization of FtsH1 in the cytoplasmic membrane and FtsH3 in both thylakoid and

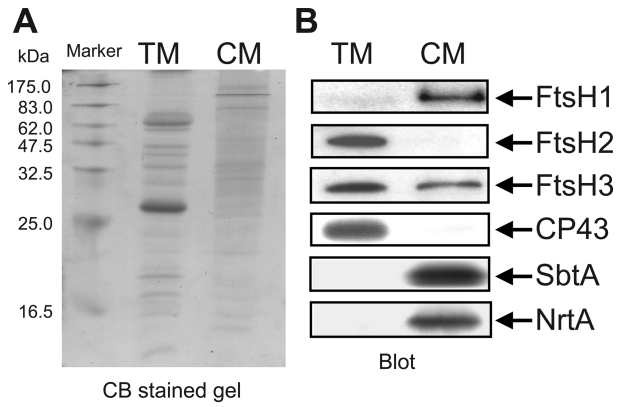

Fig. 12. Localization of FtsH1-3 in purified thylakoid and cytoplasmic membranes.
A. Coomassie stained gel of thylakoid (TM) and cytoplasmic membranes (CM).
B. Immunochemical detection of proteins was performed using antibodies specific for FtsH1, FtsH2, FtsH3, for thylakoid marker CP43 and cytoplasmic membrane markers SbtA and NrtA, transporters of bicarbonate and nitrate respectively. 1 μg of proteins was loaded for each membrane sample.

cytoplasmic membranes (Fig. 12). Thus, we conclude that the FtsH1/FtsH3 complex is localized in the cytoplasmic membrane.

Discussion

Previous studies have provided an extensive analysis of possible regulators of iron homeostasis in cyanobacterial model organisms (Ghassemian and Straus, 1996; Kunert *et al.*, 2003; Hernández-Prieto *et al.*, 2012; González *et al.*, 2014). A complex iron regulatory network has been proposed involving the Fur repressor which acts at the transcriptional level (González *et al.*, 2012) and small regulatory RNAs at the post-transcriptional level (Dühring *et al.*, 2006; Sevilla *et al.*, 2011). Nevertheless, the possibility that the abundance of Fur could be regulated by proteolysis has not yet been examined either in cyanobacteria or in other bacteria.

FtsH is known to control the level of some regulatory cytosolic proteins like heat shock proteins and transcriptional factors. For instance, *E. coli* FtsH is involved in rapid degradation of the heat shock sigma factor, sigma32 (RpoH), under non-stress conditions *in vivo* (Urech *et al.*, 2000). In the case of *Synechocystis* 6803, FtsH2 (encoded by *slr0228*) is involved in acclimation to low carbon conditions via regulation of the level of NdhR which is a transcriptional repressor controlling transcription of genes required for induction of carbon-concentrating mechanisms (Zhang *et al.*, 2007). Since FtsH2 has been found to exist as a hetero-oligomeric complex with FtsH3 *in vivo*, we assume that the FtsH2/FtsH3 complex is responsible for this regulatory process (Boehm *et al.*, 2012).

In the present study we studied the role of FtsH complexes in the regulation of the cellular level of the Fur repressor. We tested the acclimation to iron depletion in various strains mutated in FtsH proteases and found that the absence of FtsH2 and FtsH4 (not shown) did not significantly affect the process. On the other hand, we noticed that mutants with suppressed expression of the essential FtsH1 and FtsH3 proteases were not able to acclimate to iron depletion via expression of proteins whose synthesis is normally induced under iron deficiency. We tested several expression systems used for downregulation of gene expression in bacteria and the required low level of expression of *ftsH1* and *ftsH3* was achieved using promoters downregulated by Cu^{2+} ions and ammonia respectively. In contrast, the suppression of *ftsH* genes was not sufficient using the tetracycline controlled promoter (Huang and Lindblad, 2013). One potential disadvantage of our approach is that the concentrations of Cu^{2+} ions and ammonia used could have adverse effects on cyanobacterial photosynthesis (Drath *et al.*, 2008; Deng *et al.*, 2014). Indeed, the cells grown in the presence of ammonia did show symptoms of stress as reflected by the increased level of carotenoids (Fig. 2A). Nevertheless, as the mutant strains were always compared with the control strains cultivated under exactly the same conditions, any differences identified between the control strains and corresponding suppression mutants could be ascribed to the specific effect on gene regulation, not a general effect of the regulating substances.

Given the recent identification of FtsH1/FtsH3 complexes (Boehm *et al.*, 2012), the results indicate that induction of the *isiA/isiB* operon and other iron responsive genes examined depends not only on the abundance of iron but also on the level of the FtsH1/FtsH3 complex which determines the amount of the Fur repressor. Microarray data showed no significant changes in the level of Fur transcript in WT and FtsH3down strains during iron depletion excluding the transcriptional regulation of Fur level (Krynicka and Hess, unpublished). It is evident that the FtsH1/FtsH3 protease is superordinate to Fur in the regulatory cascade of iron homeostasis. Although we do not have evidence that the regulation is mediated by direct degradation of Fur by the protease complex, this scenario is highly probable. Given that Fur can be present in the cytoplasm, this would mean that the proteolytic domains of the FtsH1/FtsH3 complexes are also oriented on the cytoplasmic side of the membrane (Lee *et al.*, 2011; Boehm *et al.*, 2012).

The localization of the majority of Fur to the membrane fraction in a form that is unable to be solubilized by DDM is rather surprising. Since we were not able to remove the protein from membranes using DFB, the binding is not dependent on iron. Fur was released from the membrane fraction using 0.1 M sodium carbonate which is known to

efficiently wash out peripheral membrane-associated proteins but not transmembrane ones (Fujiki *et al*., 1982). Fur could also be solubilized by SDS or, alternatively, by DDM in the presence of EDTA suggesting the role of divalent cations in Fur binding. In this respect, Fur behaves like the Slr0006 protein induced under carbon-limiting conditions (Carmel *et al*., 2011), possibly because both proteins are present in a similar compartment. In the same DDM-unsolubilized fraction we also detected the LexA transcription factor by mass spectrometry (not shown). This factor has been shown to colocalize with DNA by Oliveira and Lindblad (2011) and has also been detected in cytoplasmic membrane fractions (Zhang *et al*., 2009). Likewise, Fur has also been detected in the purified cytoplasmic membrane of *Synechocystis* (Tiago Selao, personal communication). Taking into account the cytoplasmic membrane location of the FtsH1/FtsH3 complex, we speculate that Fur (and possibly other transcriptional factors like LexA) mediates the interaction of the membrane with DNA. When Fur detaches from DNA in the absence of iron, Fur becomes accessible to the FtsH1/FtsH3 complex and is degraded. Membrane association of Fur bound to DNA might be physiologically relevant and reflect the tight coupling of transcription and translation of membrane proteins. This would explain why a membrane-bound protease such as FtsH1/FtsH3 is involved in regulating the level of Fur rather than a soluble protease.

Our concept of FtsH1/FtsH3-mediated regulation of iron homeostasis in *Synechocystis 6803* can be summarized in the following way. In WT at sufficient iron concentrations Fe^{2+} binds to the regulatory site of the Fur monomer and triggers conformational changes leading to an increase in Fur binding affinity for specific DNA sequences in the promoter regions of *isiA/isiB* and other Fur-regulated operons (Pohl *et al*., 2003; Pecqueur *et al*., 2006). The activated Fur becomes attached to these so-called Fur boxes and transcription of the *isiA/isiB* operon is repressed (Hantke, 2001; McHugh *et al*., 2003). When the intracellular iron concentration decreases, Fur loses its bound Fe^{2+}, detaches from the Fur box and *isiA/isiB* genes start to be transcribed. Assuming an equilibrium between DNA-bound and unbound repressor, degradation of detached Fur by FtsH1/FtsH3 would help drive the detachment of Fur from DNA. Under conditions of iron sufficiency, the situation in the FtsH3down and FtsH1down mutants is similar to that in WT. Fur is attached to DNA and expression of IsiA is repressed. The level of detached Fur is just slightly higher in comparison to the WT cells. A different situation occurs upon iron depletion. Fur loses its bound iron and largely detaches from the promoter region. In mutants containing reduced levels of the FtsH1/FtsH3 complex, Fur released from DNA is not degraded and accumulates in the membrane fraction. This increases the probability of scavenging the residual amount of iron in the cells keeping the level of iron-bound Fur high enough for sufficient binding to the Fur boxes. Alternatively, the iron-free Fur despite its lower affinity to DNA can weakly and transiently bind to the Fur box keeping the regulated genes suppressed. Indeed, DNase I footprinting analysis has indicated that binding of Fur to DNA and therefore the expression level of iron-controlled genes is a function of the concentration of both the Fur protein and its cognate metal ion. A higher Fur concentration in the absence of metals afforded approximately the same footprint as lower concentration of Fur in presence of metal ion (de Lorenzo *et al*., 1987; Coy and Neilands, 1991).

Expression of IsiA, as well as some other proteins hypothetically regulated by Fur, increases in *Synechocystis* not only under iron depletion but also under other conditions such as mutation of PSI (Jeanjean *et al*., 2003), stationary growth phase (Singh and Sherman, 2006) and high concentrations of hydrogen peroxide (Singh *et al*., 2005) or cadmium (Houot *et al*., 2007). This type of regulation can be nicely explained by the increased accumulation of FtsH proteases under these conditions (Houot *et al*., 2007) which would suppress the level of Fur thereby allowing expression of IsiA even in the presence of iron.

Although our previous data indicated that FtsH3 was able to form heterocomplexes with either FtsH1 or FtsH2 (Boehm *et al*., 2012), we were unable to assess whether FtsH3 was also able to form homocomplexes. Analysis of mutants (Fig. 10) and changes in the level of FtsH proteases during iron depletion (Figs 8 and S1) suggest that the vast majority of FtsH1-3 is present as FtsH1/FtsH3 and FtsH2/FtsH3 heterocomplexes, and that the level of the homocomplexes, if present, is much lower. However, we still consider it possible that the composition of FtsH complexes is dynamic and that under certain growth or stress conditions homocomplexes might accumulate to some extent.

Our previous analysis of an FtsH2 null mutant also indicated that levels of FtsH3 declined to approximately 10% of WT levels suggesting that the amount of the FtsH1/FtsH3 complex was much less than the FtsH2/FtsH3 complex (Boehm *et al*., 2012). Consistent with this, downregulation of FtsH1 did not result in drastic depletion of FtsH2 and FtsH3; indeed the level of FtsH2 and FtsH3 actually increased during iron starvation. However, the FtsH1down mutant did show weaker symptoms of iron depletion than FtsH3down, despite the low levels of FtsH1 and FtsH3 (Fig. S1A and Fig. 8 respectively). Consequently, we cannot rule out that the FtsH2/FtsH3 complex can substitute to a limited extent for the FtsH1/FtsH3 complex in controlling the level of Fur. The parallel increase in FtsH2 and FtsH3 levels in the FtsH1over strain (Fig. 9B)

is interesting and might reflect upregulated expression of the FtsH2/FtsH3 complex in response to increased availability of FtsH3 if expression of FtsH3 is increased in response to enhanced FtsH1 levels. Alternatively increased levels of FtsH2/FtsH3 might be a response to some other signal caused by overexpression of FtsH1.

The presence of FtsH3 in FtsH heterocomplexes found in either the cytoplasmic or thylakoid membranes raises important questions about how sorting of FtsH3 is achieved. The relationship between the cytoplasmic and thylakoid membrane and their possible contacts is currently unclear in cyanobacteria. One possibility is that both membrane compartments share a common origin allowing competition between FtsH heterocomplexes for the shared subunit.

In summary, it seems that the co-ordinated expression of the Fur regulated genes in *Synechocystis* is more complex than was originally thought. Such convoluted regulatory mechanisms enable the cell to cope with various environmental changes. Homologues of Fur and FtsH1 and FtsH3 are encoded in the genomes of all cyanobacterial species so far examined (see Cyanobase) and so we believe that FtsH-mediated control of Fur expression operates in other cyanobacterial species including the primordial cyanobacterium *Gloeobacter violoceus*. Indeed, we have also observed a similar cellular location of Fur and its depletion during iron deprivation in the cyanobacterium *Anabaena* PCC 7120 (not shown). Since the Fur repressor is also involved in the regulation of iron homeostasis in other bacteria, it will be interesting to establish whether the role of the FtsH protease in the regulation of the Fur level is conserved within the whole eubacterial kingdom.

Experimental procedures

Strains, their construction and cultivation

The previously described FtsH3down (originally termed SynFtsH3reg, Boehm *et al*., 2012) and FtsH2-less (FtsH2$^-$) strains (Komenda *et al*., 2006) as well as the control wild type (WT) strain were derived from the non-motile glucose-tolerant *Synechocystis* sp. PCC 6803 strain obtained from the laboratory of Wim Vermaas. Downregulation of FtsH3 was studied in cultures cultivated in the presence of ammonium ions as described in (Boehm *et al*., 2012). To deplete iron the cells were transferred to iron depleted medium (residual concentration of iron about 5 μM) supplemented with 10 μM deferoxamin B (DFB), an iron chelator. Cells were cultivated in the presence of 5 mM glucose at an irradiance of 10 μmol photons m^{-2} s^{-1} of white light.

For construction of the FtsH1down strain the *ftsH1* (*slr1390*) gene was cloned into the pSK9 vector (Kuchmina *et al*., 2012) used for conditional knockouts of genes fused to the *petJ* promoter which is repressed by copper. The resulting integrative plasmid (Fig. S4A) was used for transformation of the WT strain of *Synechocystis* 6803 via homologous recombination. Transformants were selected for chloramphenicol resistance (30 μg ml^{-1}) and complete segregation was confirmed by PCR. The wild-type copy of the *ftsH1* (*slr1390*) was deleted using a linear construct containing upstream and downstream regions of the *ftsH1* (*slr1390*) gene with the kanamycin resistance cassette in the middle generated by megaprimer PCR method (Burke and Barik, 2003) as described in detail in Supplementary Material and Methods and Fig. S4B. Successful deletion of original *ftsH1* indicated that FtsH1 is functionally expressed using the *petJ* promoter. To suppress expression of FtsH1, the strain was initially grown in BG-11 medium lacking copper ions and after reaching OD_{750} of 0.5 (exponential phase of growth) copper ions were added to give a final concentration 0.8 μM (BG11Cu+ medium). For iron depletion treatment the cells were transferred to the BG11Cu+ medium lacking ferric ions supplemented with 20 μM DFB. The mutant was cultivated in with the presence of 5 mM glucose at an irradiance of 10 μmol photons m^{-2} s^{-1} of white light.

For construction of the FtsH1over strain the *ftsH1* gene was cloned into the pPD-FLAG vector (Hollingshead *et al*., 2012), normally used for expression of 3xFLAG-tagged protein under the strong *psbA2* promoter. In our construct the FLAG tag was omitted (Fig. S5A). *Synechocystis* 6803 transformants were selected for kanamycin resistance (50 μg ml^{-1}). The wild-type copy of *ftsH1* (*slr1390*) was again deleted using a linear deletion construct generated by megaprimer PCR method, this time containing a chloramphenicol-resistance cassette (Fig. S5B). The segregated mutant was cultivated autotrophically in standard BG-11 medium at an irradiance of 40 μmol photons m^{-2} s^{-1} of white light.

The FtsH2/FtsH4-less double mutant termed FtsH2$^-$/FtsH4$^-$ used for identification of the FtsH1/FtsH3 complex was constructed by transformation of the existing FtsH2$^-$ strain by an *ftsH4* knockout vector (Fig. S6A) as described in detail in Supplementary Material and Methods. The double mutant was selected for resistance to both chloramphenicol (30 μg ml^{-1}) and kanamycin (5 μg ml^{-1}) and was grown under low-light conditions (~ 5 μmol photons m^{-2} s^{-1}) until segregation was complete as judged by PCR. The absence of the FtsH4 protein was verified by immunoblotting (Fig. S6B). The mutant was cultivated in BG-11 medium supplemented with 5 mM glucose at an irradiance of 10 μmol photons m^{-2} s^{-1} of white light.

GFP-tagged FtsH mutants were constructed using transformation vectors consisting of the particular *ftsH* coding sequence fused to DNA encoding a thrombin cleavage site, GFP and a strep II tag with a downstream selectable marker conferring chloramphenicol resistance constructed as described in detail in Supplementary Material and Methods and in Fig. S7. After transformation of WT, transformants were selected for chloramphenicol resistance (30 μg ml^{-1}) and complete segregation was confirmed by PCR. The resulting mutants are termed FtsHxGFP, where FtsHx represents the particular FtsH subunit. The strains were cultivated autotrophically in standard BG-11 medium at an irradiance of 40 μmol photons m^{-2} s^{-1} of white light.

All liquid cultures (50–100 ml) were shaken in 250 ml conical flasks at 29°C. Cultures were analysed in the exponential phase (OD_{750} in the range 0.5–0.7). All experiments and measurements with cells were performed at least in triplicate (biological repeats) and typical results are shown in the figures.

Analysis of proteins and their complexes

Membrane protein complexes were analysed by clear native electrophoresis in combination with SDS-PAGE and Western blotting as described in Komenda *et al*. (2012). The previously described primary antibodies against the following proteins were used in this study: anti-FtsH2 and anti-FtsH3 described in (Boehm *et al*., 2012), anti-PsaD (Shen and Bryant, 1995), anti-IsiA (Sandström *et al*., 2001), anti-Fur (Hernández *et al*., 2002), anti-CP43 (Boehm *et al*., 2009), anti-SbtA (Boehm *et al*., 2009) and anti-NrtA (Norling *et al*., 1998). We also used new antibodies raised in rabbit against peptide 578–592 and 556–573 of the *Synechocystis* 6803 FtsH1 and FtsH4 proteins, respectively, against peptide 2–18 of the *Synechocystis* 6803 PsaA protein and against peptide 147–160 of *Synechocystis* 6803 PilA1. Purified plasma and thylakoid membrane fractions from *Synechocystis* cells were prepared by aqueous polymer two-phase partitioning in combination with sucrose density centrifugation (Norling *et al*., 1998).

Tryptic in-gel digestion and protein identification by mass spectrometry

The identification of the Coomassie Blue-stained protein spot separated by 2D CN/SDS-PAGE were done after tryptic digestion on a NanoAcquity UPLC (Waters) on-line coupled to an ESI Q-ToF Premier mass spectrometer (Waters) as described in (Janouškovec *et al*., 2013).

Spectroscopic methods

Absorption spectra were measured using a Shimadzu UV3000 spectrophotometer (Komenda *et al*., 2007).

Fluorescence microscopy

Fluorescence micrographs were obtained with a laser-scanning confocal microscope Olympus FV1000 (Olympus, Japan) using procedures described in detail in Supplementary Material and Methods. GFP fluorescence was measured between 500–530 nm (with emission dichroic mirror reflecting below 560 nm) and Chl fluorescence between 690–790 nm. Series of 20 images were taken for every sample and after their averaging the GFP and Chl differences across the cell were calculated to quantify GFP localization.

RNA isolation, reverse transcription and quantitative PCR

Total RNA was isolated from frozen cells following the hot Trizol protocol as described in (Komenda *et al*., 2007), purified by an RNeasy MinElute Cleanup Kit (Qiagen) and treated with TURBO DNase (Ambion). 20 ng of purified RNA was used for cDNA synthesis using specific primers for *isiA* and *slr1295* and SuperScript II Reverse Transcriptase (Invitrogen). Real time-quantitative PCR reactions were performed on a Rotor-Gene 3000 using the iQ SYBR Green Supermix (Bio-Rad). Determination of the *isiA* and *slr1295* transcript levels by quantitative PCR was performed in triplicate using three independent cultures. *rnpB* (encoding the B subunit of ribonuclease P) was used as a reference gene. Its level was found to be proportional to total RNA (measured spectrophotometrically) in all strains. The ΔΔCt method was used to calculate gene expression normalized against *rnpB*. The ΔCt values were reproducible to within 0.5 cycle.

Acknowledgements

Authors are grateful to Barbora Zemanová for excellent technical assistance and Maria Fillat for antibody against Fur. V. K, J. K. and R. K. were supported by projects Algatech (CZ.1.05/2.1.00/03.0110), RVO61388971 and P501/12/G055 of the Grant Agency of the Czech Republic, and J.Y. and P.J.N. were supported by the UK Biotechnology and Biological Sciences Research Council (grant BB/F020554/1).

References

Bagg, A., and Neilands, J.B. (1987) Ferric uptake regulation protein acts as a repressor, employing iron(II) as a cofactor to bind the operator of an iron transport operon in *Escherichia coli*. *Biochemistry* **26:** 5471–5477.

Bibby, T.S., Nield, J., and Barber, J. (2001a) Iron deficiency induces the formation of an antenna ring around trimeric photosystem I in cyanobacteria. *Nature* **412:** 743–745.

Bibby, T.S., Nield, J., and Barber, J. (2001b) Three-dimensional model and characterization of the iron stress-induced CP43′-photosystem I supercomplex isolated from the cyanobacterium *Synechocystis* PCC 6803. *J Biol Chem* **276:** 43246–43252.

Boehm, M., Nield, J., Zhang, P., Aro, E.-M., Komenda, J., and Nixon, P.J. (2009) Structural and mutational analysis of band 7 proteins in the cyanobacterium *Synechocystis* PCC 6803. *J Bacteriol* **191:** 6425–6435.

Boehm, M., Yu, J., Krynicka, V., Barker, M., Tichy, M., Komenda, J., *et al*. (2012) Subunit organization of a *Synechocystis* hetero-oligomeric thylakoid FtsH complex involved in Photosystem II repair. *Plant Cell* **24:** 3669–3683.

Breitbarth, E., Achterberg, E.P., Ardelan, M.V., Baker, A.R., Bucciarelli, E., Chever, F., *et al*. (2010) Iron biogeochemistry across marine systems – progress from the past decade. *Biogeosciences* **7:** 1075–1097.

Burke, E., and Barik, S. (2003) Megaprimer PCR: application in mutagenesis and gene fusion. *Methods Mol Biol* **226:** 525–532.

Burnap, R.L., Troyan, T., and Sherman, L.A. (1993) The highly abundant chlorophyll-protein complex of iron-deficient *Synechococcus* sp. PCC7942 (CP43′) is encoded by the *isiA* gene. *Plant Physiol* **103:** 893–902.

Carmel, D., Mulo, P., Battchikova, N., and Aro, E.-M. (2011) Membrane attachment of Slr0006 in *Synechocystis* sp. PCC 6803 is determined by divalent ions. *Photosynth Res* **108:** 241–245.

Coy, M., and Neilands, J.B. (1991) Structural dynamics and functional domains of the Fur protein. *Biochemistry* **30:** 8201–8210.

Crosa, J.H. (1997) Signal transduction and transcriptional and posttranscriptional control of iron-regulated genes in bacteria. *Microbiol Mol Biol Rev* **61:** 319–336.

Deng, C., Pan, X., Wang, S., and Zhang, D. (2014) Cu^{2+} inhibits Photosystem II activities but enhances Photosystem I quantum yield of Microcystis aeruginosa. *Biol Trace Elem Res* **160:** 268–275.

Dian, C., Vitale, S., Leonard, G.A., Bahlawane, C., Fauquant, C., Leduc, D., *et al*. (2011) The structure of the *Helicobacter pylori* ferric uptake regulator Fur reveals three functional metal binding sites. *Mol Microbiol* **79:** 1260–1275.

Drath, M., Kloft, N., Batschauer, A., Marin, K., Novak, J., and Forchhammer, K. (2008) Ammonia triggers photodamage of Photosystem II in the cyanobacterium *Synechocystis* sp. strain PCC 6803. *Plant Physiol* **147:** 206–215.

Dühring, U., Axmann, I.M., Hess, W.R., and Wilde, A. (2006) An internal antisense RNA regulates expression of the photosynthesis gene *isiA*. *Proc Natl Acad Sci USA* **103:** 7054–7058.

Erzberger, J.P., and Berger, J.M. (2006) Evolutionary relationships and structural mechanisms of AAA+ proteins. *Annu Rev Biophys Biomol Struct* **35:** 93–114.

Escolar, L., de Lorenzo, V., and Pérez-Martín, J. (1997) Metalloregulation *in vitro* of the aerobactin promoter of *Escherichia coli* by the Fur (ferric uptake regulation) protein. *Mol Microbiol* **26:** 799–808.

Escolar, L., Pérez-Martín, J., and de Lorenzo, V. (1999) Opening the iron box: transcriptional metalloregulation by the Fur protein. *J Bacteriol* **181:** 6223–6229.

Fujiki, Y., Hubbard, A.L., Fowler, S., and Lazarow, P.B. (1982) Isolation of intracellular membranes by means of sodium carbonate treatment: application to endoplasmic reticulum. *J Cell Biol* **93:** 97–102.

Garcin, P., Delalande, O., Zhang, J.-Y., Cassier-Chauvat, C., Chauvat, F., and Boulard, Y. (2012) A transcriptional-switch model for Slr1738-controlled gene expression in the cyanobacterium *Synechocystis*. *BMC Struct Biol* **12:** 1.

Ghassemian, M., and Straus, N.A. (1996) Fur regulates the expression of iron-stress genes in the cyanobacterium *Synechococcus* sp. strain PCC 7942. *Microbiology* **142:** 1469–1476.

Ghassemian, M., Lutes, J., Tepperman, J.M., Chang, H.S., Zhu, T., Wang, X., *et al*. (2006) Integrative analysis of transcript and metabolite profiling data sets to evaluate the regulation of biochemical pathways during photomorphogenesis. *Arch Biochem Biophys* **448:** 45–59.

González, A., Bes, M.T., Valladares, A., Luisa Peleato, M., and Fillat, M.F. (2012) FurA is the master regulator of iron homeostasis and modulates the expression of tetrapyrrole biosynthesis genes in *Anabaena* sp. PCC 7120. *Environ Microbiol* **14:** 3175–3187.

González, A., Angarica, V.E., Sancho, J., and Fillat, M.F. (2014) The FurA regulon in *Anabaena* sp PCC 7120: *in silico* prediction and experimental validation of novel target genes. *Nucleic Acids Res* **42:** 4833–4846.

Guerinot, M.L., and Yi, Y. (1994) Iron: nutritious, noxious, and not readily available. *Plant Physiol* **104:** 815–820.

Guikema, J.A., and Sherman, L.A. (1983) Organization and function of chlorophyll in membranes of cyanobacteria during iron starvation. *Plant Physiol* **73:** 250–256.

Hantke, K. (2001) Iron and metal regulation in bacteria. *Curr Opin Microbiol* **4:** 172–177.

Hernández, J.A., Bes, M.T., Fillat, M.F., Neira, J.L., and Peleato, M.L. (2002) Biochemical analysis of the recombinant Fur (ferric uptake regulator) protein from *Anabaena* PCC 7119: factors affecting its oligomerization state. *Biochem J* **366:** 315–322.

Hernández, J.A., López-Gomollón, S., Muro-Pastor, A., Valladares, A., Bes, M.T., Peleato, M.L., *et al*. (2006) Interaction of FurA from *Anabaena* sp PCC 7120 with DNA: a reducing environment and the presence of Mn^{2+} are positive effectors in the binding to *isiB* and *furA* promoters. *Biometals* **19:** 259–268.

Hernández-Prieto, M.A., Schön, V., Georg, J., Barreira, L., Varela, J., Hess, W.R., *et al*. (2012) Iron deprivation in *Synechocystis*: inference of pathways, non-coding RNAs, and regulatory elements from comprehensive expression profiling. *Genes Genom Genet* **2:** 1475.

Hollingshead, S., Kopečná, J., Jackson, P.J., Canniffe, D.P., Davison, P.A., Dickman, M.J., *et al*. (2012) Conserved chloroplast open-reading frame *ycf54* is required for activity of the Magnesium protoporphyrin monomethylester oxidative cyclase in *Synechocystis* PCC 6803. *J Biol Chem* **287:** 27823–27833.

Houot, L., Floutier, M., Marteyn, B., Michaut, M., Picciocchi, A., Legrain, P., *et al*. (2007) Cadmium triggers an integrated reprogramming of the metabolism of *Synechocystis* PCC6803, under the control of the Slr1738 regulator. *BMC Genomics* **8:** 350.

Huang, H.H., and Lindblad, P. (2013) Wide-dynamic-range promoters engineered for cyanobacteria. *J Biol Eng* **7:** 10.

Huang, H.H., Parmryd, I., Nilsson, F., Persson, A.L., Pakrasi, H.B., Andersson, B., and Norling, B. (2002) Proteomics of *Synechocystis* sp. strain PCC 6803: identification of plasma membrane proteins. *Mol Cell Proteomics* **1:** 956–966.

Janouškovec, J., Sobotka, R., Lai, D.H., Flegontov, P., Konik, P., Komenda, J., *et al*. (2013) Split photosystem protein, linear-mapping topology, and growth of structural complexity in the plastid genome of *Chromera velia*. *Mol Biol Evol* **30:** 2447–2462.

Jeanjean, R., Zuther, E., Yeremenko, N., Havaux, M., Matthijs, H.C.P., and Hagemann, M. (2003) A photosystem 1 *psaFJ-null* mutant of the cyanobacterium *Synechocystis* PCC 6803 expresses the *isiAB* operon under iron replete conditions. *FEBS Lett* **549:** 52–56.

Komenda, J., Barker, M., Kuviková, S., de Vries, R., Mullineaux, C.W., Tichý, M., *et al*. (2006) The FtsH protease *slr0228* is important for quality control of Photosystem II in the thylakoid membrane of *Synechocystis* sp. PCC 6803. *J Biol Chem* **281:** 1145–1151.

Komenda, J., Tichý, M., Prášil, O., Knoppová, J., Kuviková, S., Vries, R., *et al*. (2007) The exposed N-terminal tail of the D1 subunit is required for rapid D1 degradation during Photosystem II repair in *Synechocystis* sp PCC 6803. *Plant Cell* **19:** 2839–2854.

Komenda, J., Knoppová, J., Kopečná, J., Sobotka, R., Halada, P., Yu, J., *et al*. (2012) The Psb27 assembly factor binds to the CP43 complex of Photosystem II in the cyanobacterium *Synechocystis* sp. PCC 6803. *Plant Physiol* **158:** 476–486.

Kuchmina, E., Wallner, T., Kryazhov, S., Zinchenko, V.V., and Wilde, A. (2012) An expression system for regulated protein production in *Synechocystis* sp PCC 6803 and its application for construction of a conditional knockout of the ferrochelatase enzyme. *J Biotechnol* **162:** 75–80.

Kunert, A., Vinnemeier, J., Erdmann, N., and Hagemann, M. (2003) Repression by Fur is not the main mechanism controlling the iron-inducible *isiAB* operon in the cyanobacterium *Synechocystis* sp. PCC 6803. *FEMS Microbiol Lett* **227:** 255–262.

Laudenbach, D.E., Reith, M.E., and Straus, N.A. (1988) Isolation, sequence analysis, and transcriptional studies of the flavodoxin gene from *Anacystis nidulans* R2. *J Bacteriol* **170:** 258–265.

Lee, S., Augustin, S., Tatsuta, T., Gerdes, F., Langer, T., and Tsai, F.T.F. (2011) Electron cryomicroscopy structure of a membrane-anchored mitochondrial AAA protease. *J Biol Chem* **286:** 4404–4411.

Leonhardt, K., and Straus, N.A. (1994) Photosystem-II genes *isiA, psbDIC* and *psbC* in *Anabaena-7120* – cloning, sequencing and the transcriptional regulation in iron -stressed and iron-repleted cells. *Plant Mol Biol* **24:** 63–73.

Lewin, A., Moore, G.R., and Le Brun, N.E. (2005) Formation of protein-coated iron minerals. *Dalton Trans* **22:** 3597–3610.

Li, H., Singh, A.K., McIntyre, L.M., and Sherman, L.A. (2004) Differential gene expression in response to hydrogen peroxide and the putative PerR regulon of *Synechocystis* sp. Strain PCC 6803. *J Bacteriol* **186:** 3331–3345.

de Lorenzo, V., Wee, S., Herrero, M., and Neilands, J.B. (1987) Operator sequences of the aerobactin operon of plasmid ColV-K30 binding the ferric uptake regulation (Fur) repressor. *J Bacteriol* **169:** 2624–2630.

McHugh, J.P., Rodríguez-Quiñones, F., Abdul-Tehrani, H., Svistunenko, D.A., Poole, R.K., Cooper, C.E., *et al*. (2003) Global iron-dependent gene regulation in *Escherichia coli* – a new mechanism for iron homeostasis. *J Biol Chem* **278:** 29478–29486.

Mann, N.H., Novac, N., Mullineaux, C.W., Newman, J., Bailey, S., and Robinson, C. (2000) Involvement of an FtsH homologue in the assembly of functional photosystem I in the cyanobacterium *Synechocystis* sp. PCC 6803. *FEBS Lett* **479:** 72–77.

Mohamed, A., Eriksson, J., Osiewacz, H.D., and Jansson, C. (1993) Differential expression of the *psbA* genes in the cyanobacterium *Synechocystis* 6803. *Mol Gen Genet* **238:** 161–168.

Nixon, P.J., Michoux, F., Yu, J., Boehm, M., and Komenda, J. (2010) Recent advances in understanding the assembly and repair of photosystem II. *Ann Bot (Lond)* **106:** 1–16.

Norling, B., Zak, E., Andersson, B., and Pakrasi, H. (1998) 2D-isolation of pure plasma and thylakoid membranes from the cyanobacterium *Synechocystis* sp. PCC 6803. *FEBS Lett* **436:** 189–192.

Oliveira, P., and Lindblad, P. (2011) Novel insights into the regulation of LexA in the cyanobacterium *Synechocystis* sp. strain PCC 6803. *J Bacteriol* **193:** 3804–3814.

Pecqueur, L., D'Autreaux, B., Dupuy, J., Nicolet, Y., Jacquamet, L., Brutscher, B., *et al*. (2006) Structural changes of *Escherichia coli* ferric uptake regulator during metal-dependent dimerization and activation explored by NMR and x-ray crystallography. *J Biol Chem* **281:** 21286–21295.

Pisareva, T., Shumskaya, M., Maddalo, G., Ilag, L., and Norling, B. (2007) Proteomics of *Synechocystis* sp PCC 6803 – Identification of novel integral plasma membrane proteins. *FEBS J* **274:** 791–804.

Pisareva, T., Kwon, J., Oh, J., Kim, S., Ge, C.R., Wieslander, A., *et al*. (2011) Model for membrane organization and protein sorting in the cyanobacterium *Synechocystis* sp PCC 6803 inferred from proteomics and multivariate sequence analyses. *J Proteome Res* **10:** 3617–3631.

Pohl, E., Haller, J.C., Mijovilovich, A., Meyer-Klaucke, W., Garman, E., and Vasil, M.L. (2003) Architecture of a protein central to iron homeostasis: crystal structure and spectroscopic analysis of the ferric uptake regulator. *Mol Microbiol* **47:** 903–915.

Qi, Q., Hao, M., Ng, W.O., Slater, S.C., Baszis, S.R., Weiss, J.D., *et al*. (2005) Application of the *Synechococcus nirA* promoter to establish an inducible expression system for engineering the *Synechocystis* tocopherol pathway. *Appl Environ Microbiol* **71:** 5678–5684.

Ratledge, C., and Dover, L.G. (2000) Iron metabolism in pathogenic bacteria. *Annu Rev Microbiol* **54:** 881–941.

Sandström, S., Park, Y.I., Öquist, G., and Gustafsson, P. (2001) CP43′, the *isiA* gene product, functions as an excitation energy dissipator in the cyanobacterium *Synechococcus* sp. PCC 7942. *Photochem Photobiol* **74:** 431–437.

Sevilla, E., Martin-Luna, B., González, A., Gonzalo-Asensio, J.A., Luisa Peleato, M., and Fillat, M.F. (2011) Identification of three novel antisense RNAs in the *fur* locus from unicellular cyanobacteria. *Microbiology* **157:** 3398–3404.

Shcolnick, S., Summerfield, T.C., Reytman, L., Sherman, L.A., and Keren, N. (2009) The mechanism of iron homeostasis in the unicellular cyanobacterium *Synechocystis* sp. PCC 6803 and its relationship to oxidative stress. *Plant Physiol* **150:** 2045–2056.

Shen, G.Z., and Bryant, D.A. (1995) Characterization of a *Synechococcus* sp. strain PCC-7002 mutant lacking Photosystem I. Protein assembly and energy-distribution in the absence of the Photosystem I reaction center core complex. *Photosynth Res* **44:** 41–53.

Sherman, D.M., and Sherman, L.A. (1983) Effect of iron deficiency and iron restoration on ultrastructure of *Anacystis nidulans*. *J Bacteriol* **156:** 393–401.

Silva, P., Thompson, E., Bailey, S., Kruse, O., Mullineaux, C.W., Robinson, C., *et al*. (2003) FtsH is involved in the early stages of repair of Photosystem II in *Synechocystis* sp PCC 6803. *Plant Cell* **15:** 2152–2164.

Singh, A.K., and Sherman, L.A. (2000) Identification of iron-responsive, differential gene expression in the cyanobacterium *Synechocystis* sp. strain PCC 6803 with a customized amplification library. *J Bacteriol* **182:** 3536–3543.

Singh, A.K., and Sherman, L.A. (2006) Iron-independent dynamics of IsiA production during the transition to stationary phase in the cyanobacterium *Synechocystis* sp.PCC6803. *FEMS Microbiol Lett* **256:** 159–164.

Singh, A.K., and Sherman, L.A. (2007) Reflections on the function of IsiA, a cyanobacterial stress-inducible, Chl-binding protein. *Photosynth Res* **93:** 17–25.

Singh, A.K., McIntyre, L.M., and Sherman, L.A. (2003) Microarray analysis of the genome-wide response to iron deficiency and iron reconstitution in the cyanobacterium *Synechocystis* sp. PCC 6803. *Plant Physiol* **132:** 1825–1839.

Singh, A.K., Li, H., Bono, L., and Sherman, L.A. (2005) Novel adaptive responses revealed by transcription profiling of a *Synechocystis* sp. PCC 6803 Δ*isiA* mutant in the presence and absence of hydrogen peroxide. *Photosynth Res* **84:** 65–70.

Tottey, S., Patterson, C.J., Banci, L., Bertini, I., Felli, I.C., Pavelkova, A., *et al.* (2012) Cyanobacterial metallochaperone inhibits deleterious side reactions of copper. *Proc Natl Acad Sci USA* **109:** 95–100.

Tous, C., Vega-Palas, M.A., and Vioque, A. (2001) Conditional expression of RNase P in the cyanobacterium *Synechocystis* sp PCC6803 allows detection of precursor RNAs – Insight in the *in vivo* maturation pathway of transfer and other stable RNAs. *J Biol Chem* **276:** 29059–29066.

Urech, C., Koby, S., Oppenheim, A.B., Münchbach, M., Hennecke, H., and Narberhaus, F. (2000) Differential degradation of *Escherichia coli* σ^{32} and *Bradyrhizobium japonicum* RpoH factors by the FtsH protease. *Eur J Biochem* **267:** 4831–4839.

Wegener, K.M., Singh, A.K., Jacobs, J.M., Elvitigala, T., Welsh, E.A., Keren, N., *et al.* (2010) Global proteomics reveal an atypical strategy for carbon/nitrogen assimilation by a cyanobacterium under diverse environmental perturbations. *Mol Cell Proteomics* **9:** 2678–2689.

Yu, C., and Genco, C.A. (2012) Fur-mediated global regulatory circuits in pathogenic *Neisseria* species. *J Bacteriol* **194:** 6372–6381.

Zhang, L.-F., Yang, H.-M., Cui, S.-X., Hu, J., Wang, J., Kuang, T.-Y., *et al.* (2009) Proteomic analysis of plasma membranes of cyanobacterium *Synechocystis* sp strain PCC 6803 in response to high pH stress. *J Proteome Res* **8:** 2892–2902.

Zhang, P., Sicora, C.I., Vorontsova, N., Allahverdiyeva, Y., Battchikova, N., Nixon, P.J., *et al.* (2007) FtsH protease is required for induction of inorganic carbon acquisition complexes in *Synechocystis* sp. PCC 6803. *Mol Microbiol* **65:** 728–740.

Supporting information

Additional supporting information may be found in the online version of this article at the publisher's web-site.